Electronic Supplementary Material (ESI) for Chemical Communications

A New Type of Insulated Molecular Wire: A Rotaxane Derived from A Metal-Capped Conjugated Tetrayne

Nancy Weisbach, Zuzana Baranová, Sébastien Gauthier, Joseph H. Reibenspies, and John A. Gladysz*

Department of Chemistry, Texas A&M University, PO Box 30012, College Station, Texas 77842-3012, USA

General Data. Reactions were conducted under dry argon atmospheres using Schlenk techniques, but workups were carried out in air. THF was dried using a solvent dispensing system (Seca Solvent System). Hexanes, CH_2Cl_2, ethyl acetate (3 × ACS grade), I_2 (99.9%, Fisher), K_2CO_3 (99% Alfa Aesar), silica gel (Acros or Fluoroflash), and alumina (Al_2O_3, neutral, Brockmann I, for chromatography, 50-200 μm, Acros) were used as received.

NMR spectra were recorded on a Varian NMRS 500 MHz spectrometer and referenced as follows: ^{1}H NMR, residual $CHCl_3$ (δ, 7.24 ppm); $^{13}C\{^1H\}$ NMR, internal $CDCl_3$ (δ, 77.0 ppm); ^{19}F NMR, external C_6F_6 (δ, −164.9 ppm); $^{31}P\{^1H\}$ external H_3PO_4 (δ, 0.00 ppm). Melting and thermal behavior was assayed using an OptiMelt MPA 100 apparatus. IR spectra were recorded on a Shimadzu IRAffinity-1 spectrometer with a Pike MIRacle ATR system (diamond crystal). UV-visible spectra were recorded on a Shimadzu UV-1800 spectrometer. Thin-layer chromatography (TLC) was carried out on EMD Silica Gel 60 F254 or EMD Aluminum oxide 60 F254 (neutral) plates that were visualized with 254 nm or 365 nm UV light.

***trans,trans*-(C_6F_5)(*p*-tol_3P)$_2$Pt(C≡C)$_4$Pt(P*p*-tol_3)$_2$(C_6F_5)·(2,9-(1,10-phenanthrolinediyl))(*p*-$C_6H_4O(CH_2)_6O)_2$(1,3-C_6H_4) (2·3). A.** A Schlenk flask was charged with *trans*-(C_6F_5)(*p*-$tol_3P)_2Pt(C≡C)_2H$ (**1**; 0.051 g, 0.050 mmol), **3**·CuI (see text; 0.017 g, 0.021 mmol), K_2CO_3 (0.011 g, 0.083 mmol), and THF (5 mL). The suspension was warmed to 55 °C (oil bath) to give an orange solution. Then I_2 (7.7×10^{-3} M in THF, 5.0 mL, 0.039 mmol) was added dropwise with stirring over a period of 6 h. The solvent was removed by rotary evaporation. The procedure was repeated using **1** (0.054 g, 0.053 mmol), **3**·CuI (0.018 g, 0.022 mmol), K_2CO_3 (0.012 g, 0.087 mmol), THF (5 mL), and I_2 (7.7×10^{-3} M in THF, 5.0 mL, 0.039 mmol). The combined residues were chromatographed on a silica gel column (2.5 × 30 cm, packed in hexanes, eluted first with hexanes then with an ethyl acetate gradient until 1:2 v/v ethyl acetate/hexanes) to give **2·3** accompanied by the free macrocycle **3**. **B.** A round bottom flask was charged with **1** (0.099 g, 0.097 mmol), **3**·CuI (0.041 g, 0.049 mmol), K_2CO_3 (0.026 g, 0.19 mmol), and THF (20 mL). The suspension was warmed to 50 °C (oil bath) and oxygen was bubbled through the solution. The reaction was monitored via TLC (silica, 1:2 v/v ethyl acetate/hexanes). After 6 h and 14 h,

more **3**·CuI was added (0.042 g, 0.051 mmol; 0.020 g, 0.024 mmol). After 22 h (TLC showed no remaining educt) the solvent was removed by rotary evaporation. The residue was chromatographed on a silica gel column (2.5 × 30 cm, packed in hexanes, eluted first with hexanes then with an ethyl acetate gradient until 1:2 v/v ethyl acetate/hexanes) to give **2**·**3** accompanied by the free macrocycle **3**. **C.** (purification) The materials from A and B were chromatographed on an alumina column (2.5 × 30 cm, packed in hexanes, eluted first with hexanes then with an increasing CH_2Cl_2 gradient up to 10:1 v/v CH_2Cl_2/hexanes). The solvent was removed from the product containing fractions by rotary evaporation and oil pump vacuum. This gave **2**·**3** as a light yellow solid (0.025 g, 0.0093 mmol, average yield 9%), which slightly darkened at 163 °C, turned black at 277 °C, and liquefied at 281 °C. Anal. Calcd for $C_{146}H_{126}F_{10}N_2O_4P_4Pt_2$: C, 65.51; H, 4.74; N, 1.05. Found: C, 66.35; H, 5.32; N, 1.06.[s1] Subsequent fractions from the column gave **3** (0.053 g, 0.083 mmol).

NMR (δ (ppm), $CDCl_3$): ^{1}H (500 MHz) 8.43 (d, $^3J_{HH}$ = 8.7 Hz, 4H, *p*-C_6H_4), 8.28 (d, $^3J_{HH}$ = 8.7 Hz, 2H, phenanthroline), 8.12 (d, $^3J_{HH}$ = 8.4 Hz, 2H, phenanthroline), 7.76 (s, 2H, phenanthroline), 7.38-7.34 (m, 24H, *o* to P), 7.21 (t, $^3J_{HH}$ = 8.0 Hz, 1H, *m*-C_6H_4, OCCHC$\underline{H}$), 6.90 (overlapping d, $^3J_{HH}$ = 7.9 Hz, 24H, *m* to P), 6.88 (overlapping d, $^3J_{HH}$ = 8.8 Hz, 4H, *p*-C_6H_4), 6.55 (dd, $^3J_{HH}$ = 8.2 Hz, $^4J_{HH}$ = 2.1 Hz, 2H, *m*-C_6H_4, OCC$\underline{H}$CH), 6.21 (distorted t, 1H, *m*-C_6H_4, OCC$\underline{H}$CO), 3.31 (br t, $^3J_{HH}$ = 7.7 Hz, 4H, OCH_2), 3.26 (br t, $^3J_{HH}$ = 7.6 Hz, 4H, O'C'H_2), 2.10 (s, 36H, CH_3), 1.25-1.21 (m, 4H, $OCH_2C\underline{H}_2$), 1.16-1.10 (m, 4H, O'C'H_2C'$\underline{H}_2$), 0.74 (br s, 8H, $OCH_2CH_2C\underline{H}_2$); ^{13}C{^{1}H} (125 MHz)[s2] 160.6, 160.3, 156.2, 146.1 (4 s, macrocycle), 140.8 (s, *p* to P), 136.4 (s, macrocycle), 134.1 (virtual t,[s3] $^2J_{CP}$ = 6.4 Hz, *o* to P), 131.3, 129.3 (2 s, macrocycle), 128.8 (s, CH of *p*-C_6H_4),[s4] 128.5 (virtual t,[s3] $^3J_{CP}$ = 5.6 Hz, *m* to P), 127.3 (virtual t,[s3] $^1J_{CP}$ = 30.2 Hz, *i* to P), 127.2, 125.3, 118.5 (3 s, macrocycle), 114.8 (s, CH of *p*-C_6H_4),[s4] 108.5 (s, macrocycle), 100.2 (br s, Pt$\underline{C}$≡C), 96.8 (s, PtC≡$\underline{C}$), 96.7 (s, OC$\underline{C}$HCO),[s5] 67.2, 66.7 (2 s, OCH_2/O'C'H_2), 63.8 (s, PtC≡C$\underline{C}$≡C), 58.3 (s, PtC≡CC≡$\underline{C}$), 28.9, 28.7 (2 s, $OCH_2\underline{C}H_2$/O'C'H_2-$\underline{C}$'H_2), 24.8, 24.3 (2 s, $OCH_2CH_2\underline{C}H_2$/O'C'$H_2C'H_2\underline{C}$'$H_2$), 21.1 (s, CH_3); ^{31}P{^{1}H} (202 MHz) 17.76 (s, $^1J_{PtP}$ = 2660 Hz);[s6] ^{19}F (470 MHz) −116.10 (m, $^3J_{FPt}$ = 291 Hz, 2F, *o* to Pt),[s6] −163.84

(m, 2F, *m* to Pt), –164.68 (t, $^3J_{FF}$ = 19.5 Hz, 1F, *p* to Pt).

IR (ATR, cm^{-1}) 2149 m ($\nu_{C\equiv C}$), 2008 w ($\nu_{C\equiv C}$). UV-vis (nm, 4.37 × 10^{-6} M in CH_2Cl_2 (ε, $M^{-1}cm^{-1}$)) 267 (69000), 293 (120000), 325 (129000), 355 (27000), 381 (9000), 414 (5000). MS (MALDI$^+$, matrix: sinapic acid with CF_3COOK) 2714 ([**2**·**3** + K]$^+$, 2%), 2676 ([**2**·**3** + 1]$^+$, 2%), 1304 ([(tol$_3$P)(C$_6$F$_5$)Pt·**3**]$^+$, 75%), 1137 ([(tol$_3$P)Pt·**3**]$^+$, 100%), 803 ([(tol$_3$P)$_2$Pt]$^+$, 95%).

Data for **2** under identical conditions (for literature data under similar conditions, see reference 8b of text):

NMR (δ (ppm), $CDCl_3$): ^{1}H (500 MHz) 7.47-7.43 (m, 24H, *o* to P), 7.07 (d, $^3J_{HH}$ = 7.8 Hz, 24H, *m* to P), 2.34 (s, 36H, CH_3); $^{13}C\{^1H\}$ (125 MHz)[s2] 140.6 (s, *p* to P), 134.2 (virtual t,[s3] $^2J_{CP}$ = 6.4 Hz, *o* to P), 128.6 (virtual t,[s3] $^3J_{CP}$ = 5.6 Hz, *m* to P), 127.2 (virtual t,[s3] $^1J_{CP}$ = 30.2 Hz, *i* to P), 100.5 (br s, PtC≡C), 96.7 (s, PtC≡C), 64.1 (s, PtC≡CC≡C), 58.1 (s, PtC≡CC≡C), 21.3 (s, CH_3); ^{31}P (202 MHz): 17.84 (s, $^1J_{PtP}$ = 2648 Hz).[s6] IR (ATR, cm^{-1}) 2139 m ($\nu_{C\equiv C}$), 1996 w ($\nu_{C\equiv C}$). UV-vis (nm, 4.12 × 10^{-6} M in CH_2Cl_2 (ε, $M^{-1}cm^{-1}$)) 267 (61000), 275 (87000), 295 (91000), 326 (126000), 355 (8100), 383 (6000), 414 (4000).

Data for **3** under identical conditions (for literature data, see reference 9 of text):

NMR (δ (ppm), $CDCl_3$): ^{1}H (500 MHz) 8.45-8.42 (m, 4H, *p*-C$_6$H$_4$), 8.15 (d, $^3J_{HH}$ = 8.4 Hz, 2H, phenanthroline), 8.00 (d, $^3J_{HH}$ = 8.5 Hz, 2H, phenanthroline), 7.63 (s, 2H, phenanthroline), 7.17 (t, $^3J_{HH}$ = 8.2 Hz, 1H, *m*-C$_6$H$_4$, OCCHC<u>H</u>), 7.11-7.08 (m, 4H, *p*-C$_6$H$_4$), 6.55 (t, $^4J_{HH}$ = 2.3 Hz, 1H, *m*-C$_6$H$_4$, OCC<u>H</u>CO), 6.51 (dd, $^3J_{HH}$ = 8.2 Hz, $^4J_{HH}$ = 2.3 Hz, 2H, *m*-C$_6$H$_4$, OCC<u>H</u>CH), 4.05 (t, $^3J_{HH}$ = 7.0 Hz, 4H, OCH_2), 3.97 (t, $^3J_{HH}$ = 6.3 Hz, 4H, O'C'H$_2$), 1.91-1.85 (m, 4H, $OCH_2C\underline{H}_2$), 1.85-1.80 (m, 4H, O'C'H$_2$C'<u>H</u>$_2$), 1.57-1.56 (m, 8H, $OCH_2CH_2C\underline{H}_2$); $^{13}C\{^1H\}$ (125 MHz) 160.28, 160.25, 156.0, 145.8, 136.5, 131.8, 129.7 (7 s), 128.8 (s, CH of *p*-C$_6$H$_4$),[s4] 127.2, 125.3, 118.9 (3 s), 114.6 (s, CH of *p*-C$_6$H$_4$),[s4] 106.7 (s), 100.9 (s, OC<u>C</u>HCO),[s5] 67.9, 67.6 (2 s, OCH_2/O'C'H$_2$), 29.4, 28.9 (2 s, $OCH_2\underline{C}H_2$/O'C'H$_2$<u>C</u>'H$_2$), 25.82, 25.77 (2 s, $OCH_2CH_2\underline{C}H_2$/O'C'H$_2$C'H$_2$<u>C</u>'H$_2$). UV-vis (nm, 2.52 × 10^{-5} M in CH_2Cl_2 (ε, $M^{-1}cm^{-1}$)) 238 (34000), 286 (50000), 326 (25000), 339 (24000).

Data for a 1:1 mixture of **2** and **3** under identical conditions:

UV-vis (nm, **2** = 1.03 × 10^{-5} M, **3** = 1.01 × 10^{-5} M (ε, $M^{-1}cm^{-1}$)) 267 (81000), 277 (103000), 292 (106000), 325 (123000), 355 (22000), 382 (6000), 415 (3000).

Cyclic voltammetry. A BASi Epsilon potentiostat (Cell Stand C3) with the program BASi Epsilon-EC (version 2.12.77_USB) was employed. Cells were fitted with Pt working and Pt wire auxiliary electrodes, and a Ag/AgCl reference electrode containing saturated aqueous AgCl that was 3.0 M in NaCl. The CH_2Cl_2 solutions were 8.0 × 10^{-4} M in substrate, 0.10 M in *n*-Bu_4N^+ PF_6^- (Fluka, electrochemical grade, used as received), and prepared under argon. Ferrocene was subsequently added, and calibration voltammograms recorded ($E°$ = 0.46 V). The laboratory temperature was 23.0 ± 1 °C.

Crystallography. A CH_2Cl_2 solution of **2·3** was layered with hexanes and kept at room temperature. After 3 d, yellowish prisms were analyzed as outlined in Table s1. Cell parameters were obtained from 1080 frames using a 0.5° scan and refined with 9961 reflections. Integrated intensity information for each reflection was obtained by reduction of the data frames with the program SAINT.[s7] The program SADABS was used for absorption corrections.[s8] The space group was determined from systematic reflection conditions and statistical tests. The structure was solved by direct methods using SHELXTL (SHELXS).[s9] Non-hydrogen atoms were refined with anisotropic thermal parameters. Hydrogen atoms were placed in idealized positions. The parameters were refined by weighted least squares refinement on F^2 to convergence.[s9] Additional electron density was observed, and tentatively assigned to a disordered methylcyclopentane molecule (a major component of hexanes), although hexane or CH_2Cl_2 could not be excluded. Thus, the electron density contribution was extracted with the program PLATON/SQUEEZE.[s10] Two methylene carbon atoms (C127 and C128) were disordered over two positions, and refined to 0.546:0.454 occupancy ratios. Restraints were used to keep the bond distances and thermal ellipsoids chemically meaningful. Only the dominant conformation was considered in all analyses.

■ REFERENCES

(s1) This sample cannot be represented as analytically pure, but the microanalytical data are provided to illustrate the best result obtained to date. The ^{1}H and ^{13}C NMR spectra (Figures 2, s1, s2) confirm the high level of purity.

(s2) The C_6F_5 signals were not observed.

(s3) The *J* values given for the virtual triplets represent the *apparent* couplings between adjacent peaks, and not the mathematically rigorously coupling constants. See Hersh, W. H. *J. Chem. Educ.* **1997**, *74*, 1485.

(s4) This assignment was based upon peak intensity (ca. 2 × as compared to other macrocycle signals).

(s5) This chemical shift is characteristic of the CH carbon atom of resorcinol or resorcinol ethers that is flanked by CO carbon atoms: (a) Nakai, Y.; Yamada, F. *Org. Mag. Res.* **1978**, *11*, 607. (b) Makriyannis, A.; Fesik, S. *J. Am. Chem. Soc.* **1982**, *104*, 6462.

(s6) This coupling represents a satellite (d, ^{195}Pt = 33.8%), and is not reflected in the peak multiplicity given.

(s7) SAINT, "Program for Data Reduction from Area Detectors", BRUKER AXS Inc., 5465 East Cheryl Parkway, Madison, WI 53711-5373 USA.

(s8) SADABS, Sheldrick, G.M. "Program for Absorption Correction of Area Detector Frames", BRUKER AXS Inc., 5465 East Cheryl Parkway, Madison, WI 53711-5373 USA.

(s9) Sheldrick, G.M. *Acta Cryst.* **2008**, *A64*, 112.

(s10) Spek, A. L. *J. Appl. Cryst.* **2003**, *36*, 7.

Table s1: Crystallographic data for **2·3**.

empirical formula	$C_{148}Cl_4H_{130}F_{10}N_2O_4P_4Pt_2$[a]
formula weight	2846.54
temperature [K]	100(2)
diffractometer	Bruker D8 GADDS
wavelength [Å]	1.54178
crystal system	triclinic
space group	*P-1*
unit cell dimensions	
a [Å]	18.5889(8)
b [Å]	20.1664(9)
c [Å]	21.3140(10)
α [°]	117.641(3)
β [°]	93.431(3)
γ [°]	103.009
Volume [Å^3]	6770.4(5)
Z	2
ρ_{calcd} [Mg m^{-3}]	1.40
μ [mm^{-1}]	4.788
F(000)	2708
crystal size [mm^3]	0.27 × 0.22 × 0.03
range for data collection	2.38 to 60.00
Index ranges	$-20 \le h \le 20$, $-22 \le k \le 22$, $-23 \le l \le 23$
reflections collected	126786
independent reflections	19677 [R(int) = 0.0524]
max. and min. transmission	0.8697 and 0.3580
data / restraints / parameters	19677 / 15 / 1512
goodness-of-fit on F^2	1.098
Final R indices [I>2σ(I)]	*R*1 = 0.0339, *w*R2 = 0.0844
R indices (all data)	*R*1 = 0.0449, *w*R2 = 0.0880
Largest diff. peak and hole [eÅ^{-3}]	0.994 and –0.650

[a]The CH_2Cl_2 of crystallization implicit in the empirical formula and carried over to the formula weight and density has been added at the suggestion of a crystallographic reviewer; for additional comments on the nature of the solvate, see the narrative paragraph "Crystallography" in the text of the supporting information.

Table s2. Key crystallographic distances [Å] and angles [°] for **2·3** and **2**·(toluene).[a]

	2·3	**2**·(toluene)[a]
Pt1-C1	1.993(3)	1.951(5)
C1≡C2	1.207(5)	1.252(6)
C2-C3	1.358(6)	1.365(6)
C3≡C4	1.206(7)	1.209(6)
C4-C5	1.359(7)	1.351(8)
C5≡C6	1.213(6)	1.209(6)
C6-C7	1.346(5)	1.365(6)
C7≡C8	1.213(6)	1.252(6)
C8-Pt2	1.990(5)	1.951(5)
Pt1-C_{ipso}[b]	2.071(3)	2.059(4)
Pt2-C_{ipso}[b]	2.080(4)	2.059(4)
av. C_{sp}-C_{sp}	1.354	1.360
av. C_{sp}≡C_{sp}	1.210	1.231
Pt···Pt	12.8395(7)	12.895(3)
sum of bond lengths Pt1 to Pt2	12.885	12.905
P1-Pt1-P2	170.18(4)	172.28(4)
P3-Pt2-P4	174.39(4)	172.28(4)
C_{ipso}[b]-Pt1-C1	178.6(2)	177.9(2)
C8-Pt2-C_{ipso}[b]	178.6(2)	177.9(2)
Pt1-C1-C2	176.7(4)	177.6(4)
C1-C2-C3	176.0(5)	179.2(5)
C2-C3-C4	177.7(5)	177.1(5)
C3-C4-C5	177.3(5)	178.5(6)
C4-C5-C6	178.4(5)	178.5(6)
C5-C6-C7	178.9(5)	177.1(5)
C6-C7-C8	177.8(5)	179.2(5)
C7-C8-Pt2	175.7(4)	177.6(4)
average Pt-C_{sp}-C_{sp}	176.2	177.9
average C_{sp}-C_{sp}-C_{sp}	177.7	178.2
average π stacking[c]	3.847	3.688
angle stacking[d]	154.3	147.5
average sp/sp^3 distance[e]	4.207	-
average sp/sp^2 distance[f]	6.081	-
average sp/O distance[g]	5.317	-
average sp/N distance[h]	6.982	-
average sp/macrocycle distance[i]	5.439	-
closest atoms to Pt-Pt vector	C138: 3.403; C139: 3.320	-
(P1-Pt1-P2)Pt2 vs. (P3-Pt2-P4)Pt1[j]	46.4	0
(C_{ipso}-P1-Pt1-P2) vs. (P3-Pt2-P4-C_{ipso})[j]	46.8	0

C_{sp}-C_{sp} [k]	9.629	11.936

[a] Mohr, W.; Stahl, J.; Hampel, F.; Gladysz, J. A. *Chem. Eur. J.* **2003**, *9*, 3324-3340. [b] C_{ipso} is the platinum bound C_6F_5 carbon atom. [c] Average distance between midpoints of the C_6F_5 and C_6H_4R rings. [d] angle of midpoints of the three rings in *c*. [e] Average distance from every CH_2 group to the Pt-Pt vector. [f] Average distance from every C_{sp^2} atom of the 33 membered rings to the Pt-Pt vector. [g] Average distance from every oxygen atom to the Pt-Pt vector. [h] Average distance from every nitrogen atom to the Pt-Pt vector. [i] Average distance from all of the atoms in *e*-*h* to the Pt-Pt vector. [j] Angle between planes defined by these atoms on each endgroup. [k] The shortest carbon-carbon distance between parallel sp chains in the crystal lattice.

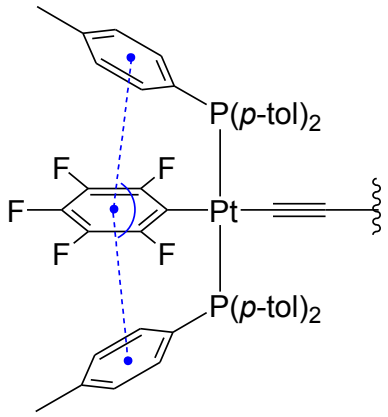

[c,d] π stacking

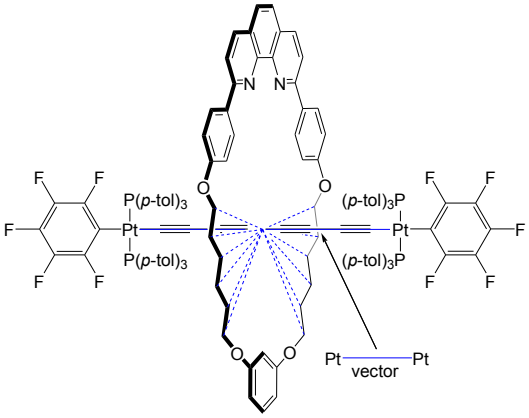

[e] average distance CH_2 groups to Pt–Pt vector

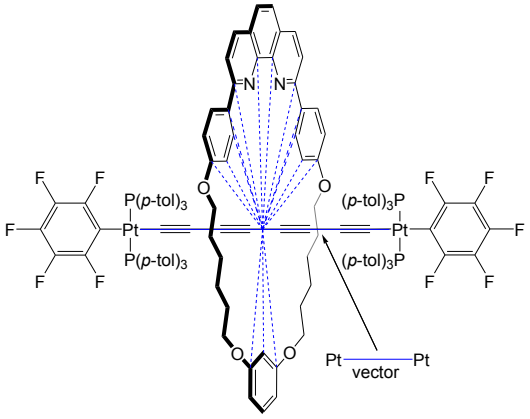

[f] average distance C_{sp^2} to Pt–Pt vector

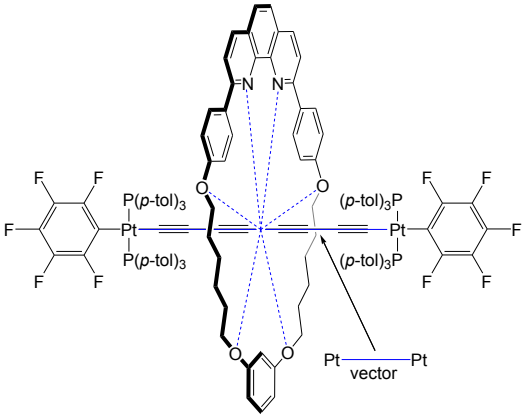

[g,h] average distance N, O atoms to Pt–Pt vector

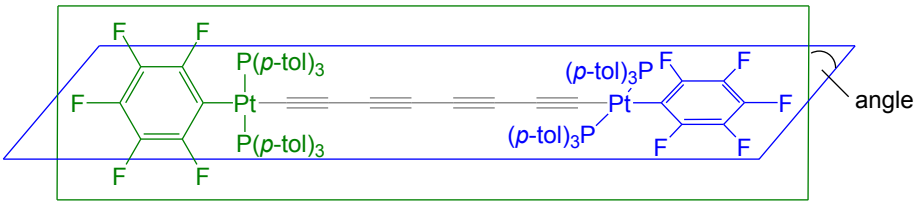

[j] angle between planes of endgroups

Table s3. Cyclic voltammetry data.

Substrate[a]	$E_{p,a}$ [V]	$E_{p,c}$ [V]	$E°$ [V]	ΔE [mV]	$i_{c/a}$
2	1.227	1.136	1.182	91	0.94
2[b]	1.261	1.143	1.202	118	0.48
3	1.403, 1.710[c]	-	-	-	0
1:1 mixture **2**:**3**[d]	1.266, 1.399	-	-	-	0[d]
2·**3**	-[e]	-	-	-	-

[a] Conditions: 8×10^{-4} M in CH_2Cl_2, n-Bu_4N^+ PF_6^-, 23.0 °C ± 1 °C; Pt working and auxiliary electrodes, Ag/AgCl reference electrode; scan rate, 100 mV s^{-1}; ferrocene, $E°$ = 0.46 V.

[b] Older data from reference Mohr, W.; Stahl, J.; Hampel, F.; Gladysz, J. A. *Chem. Eur. J.* **2003**, *9*, 3324-3340; as the sample for the present study was repeatedly crystallized, the $i_{c/a}$ value progressively increased. Conditions: (7 - 9) × 10^{-4} M in CH_2Cl_2, n-Bu_4N^+ BF_4^-, 22.5 °C ± 1 °C; Pt working and counter electrodes, Ag wire pseudoreference electrode; scan rate, 100 mV s^{-1}; ferrocene, $E°$ = 0.46 V.

[c] The onset of another peak is apparent with further anodic scaning.

[d] When the switching potential is shifted to 1.350 V (prior to reaching the second anodic peak), the first oxidation becomes partially reversible, with an $i_{c/a}$ value of 0.66.

[e] See Figure s4.

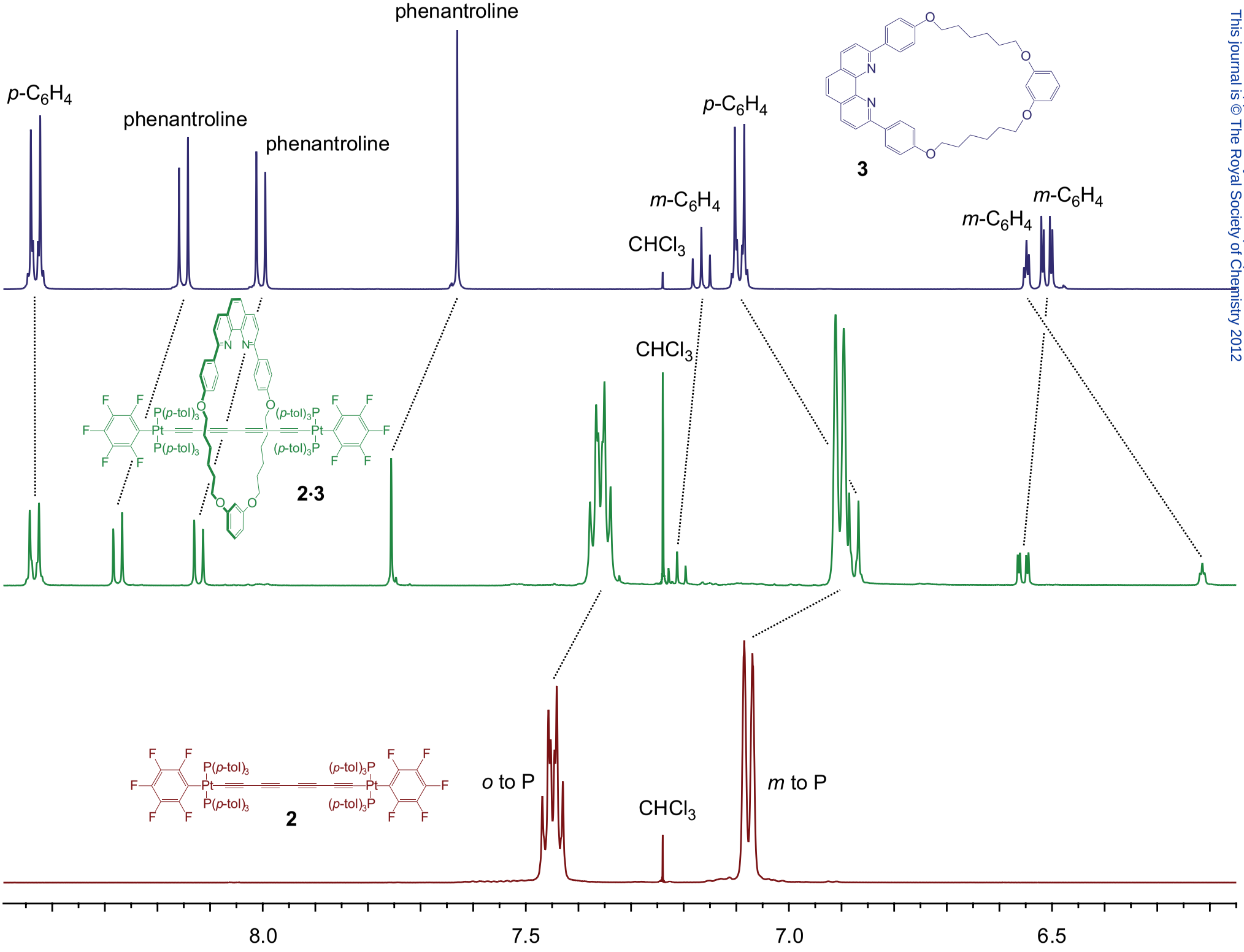

Figure s1. Additional shifts in ^{1}H NMR signals upon rotaxane formation.

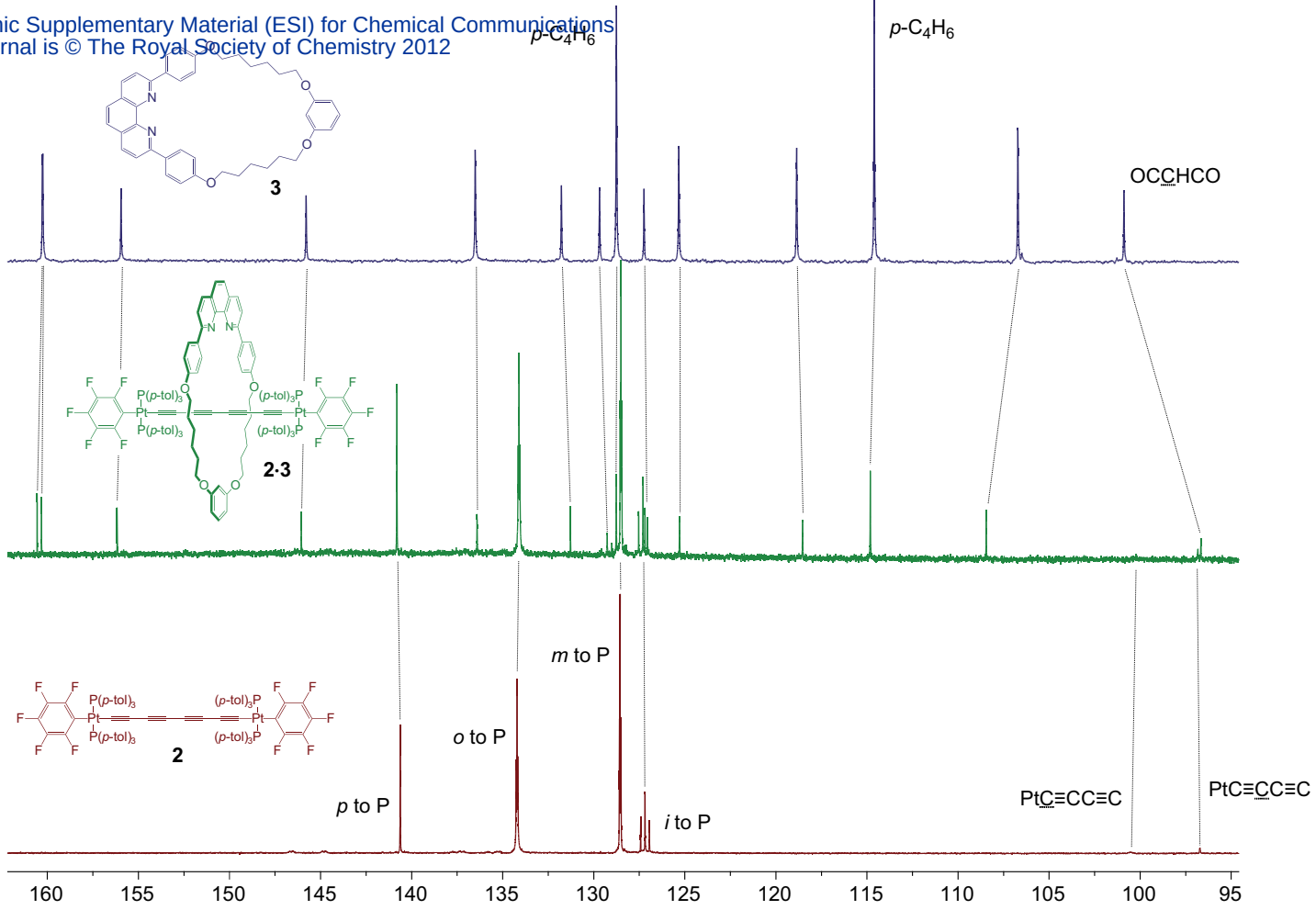

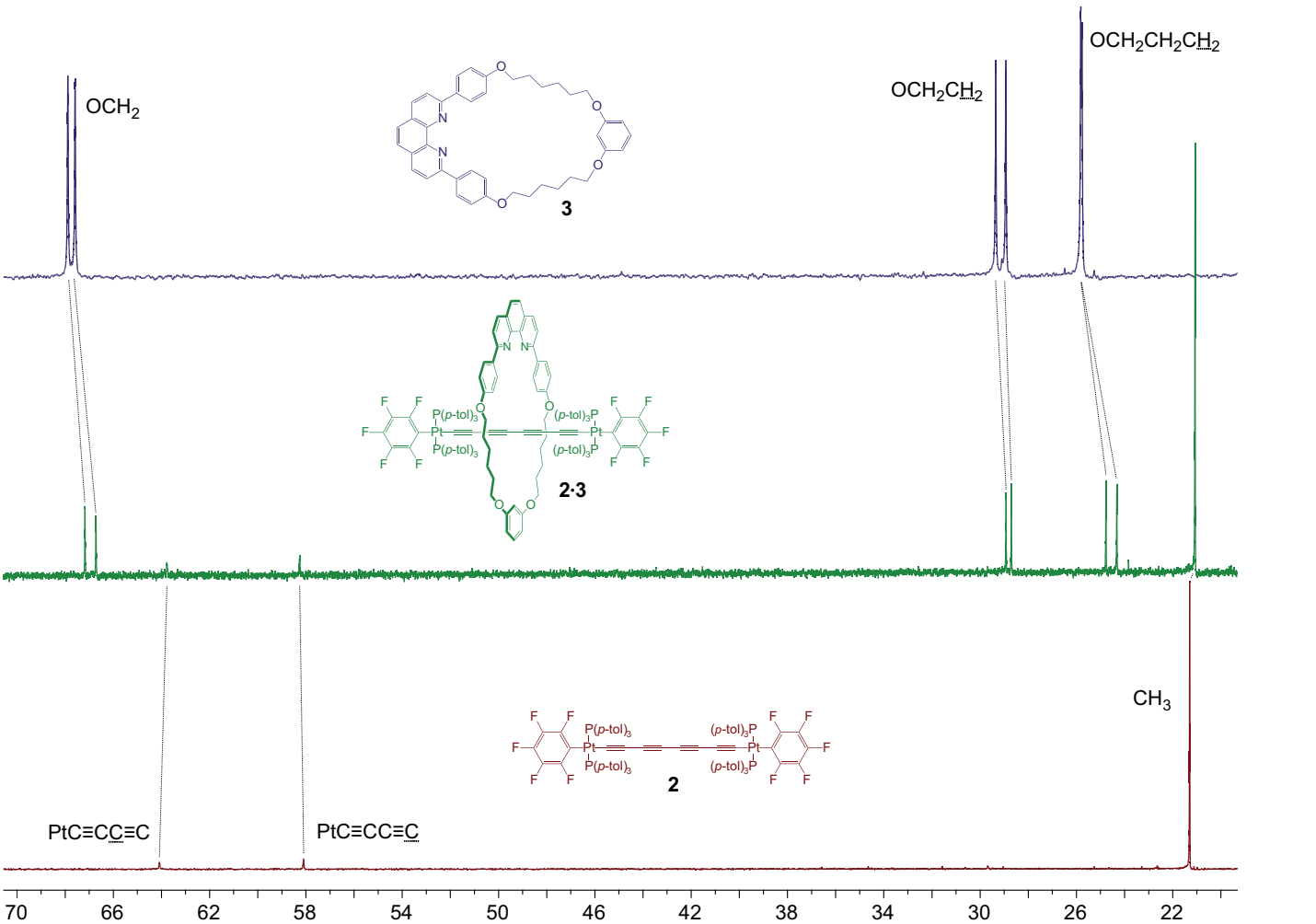

Figure s2. Shifts in ^{13}C NMR signals upon rotaxane formation.

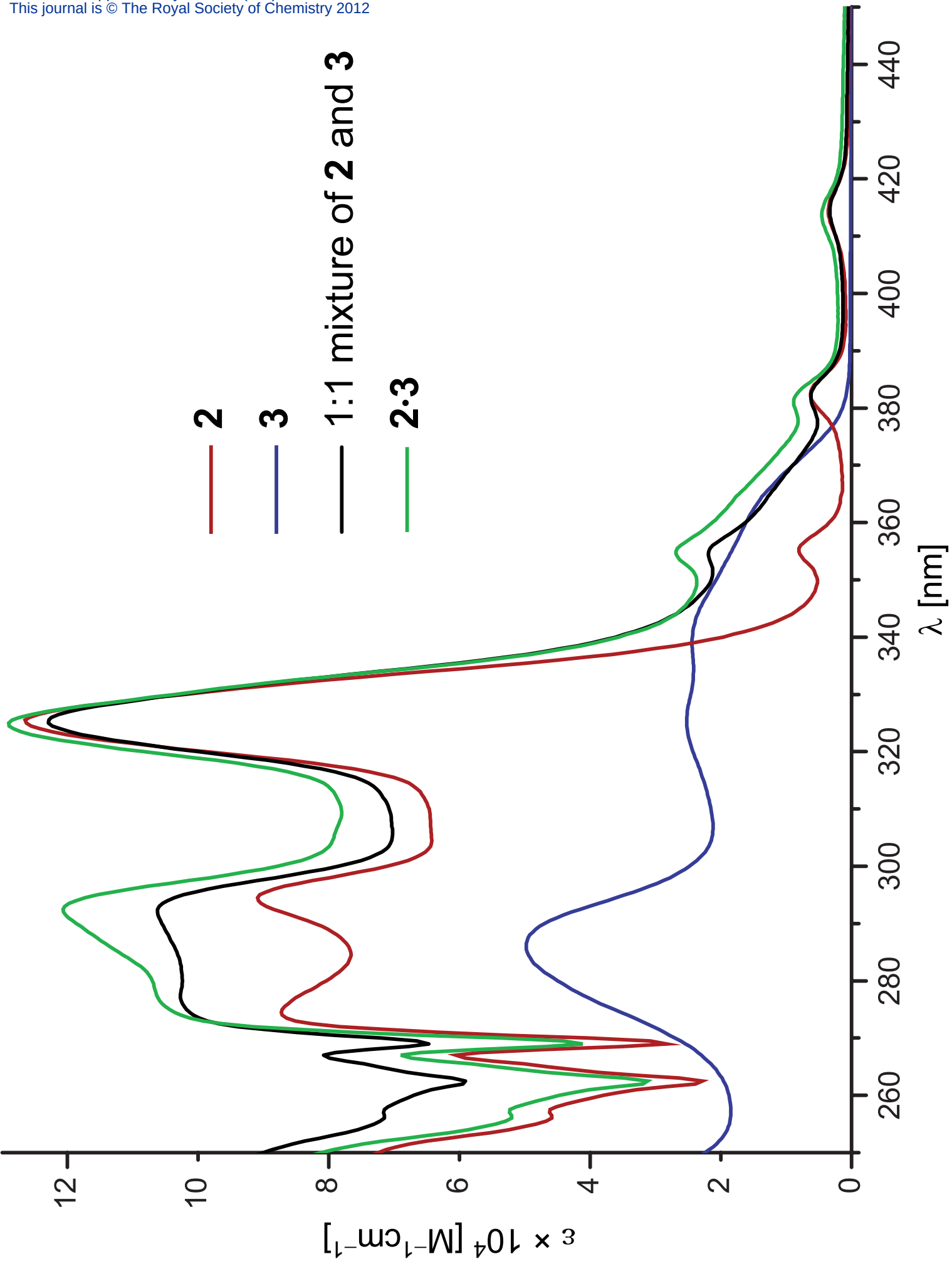

Figure s3. UV-visible spectra.

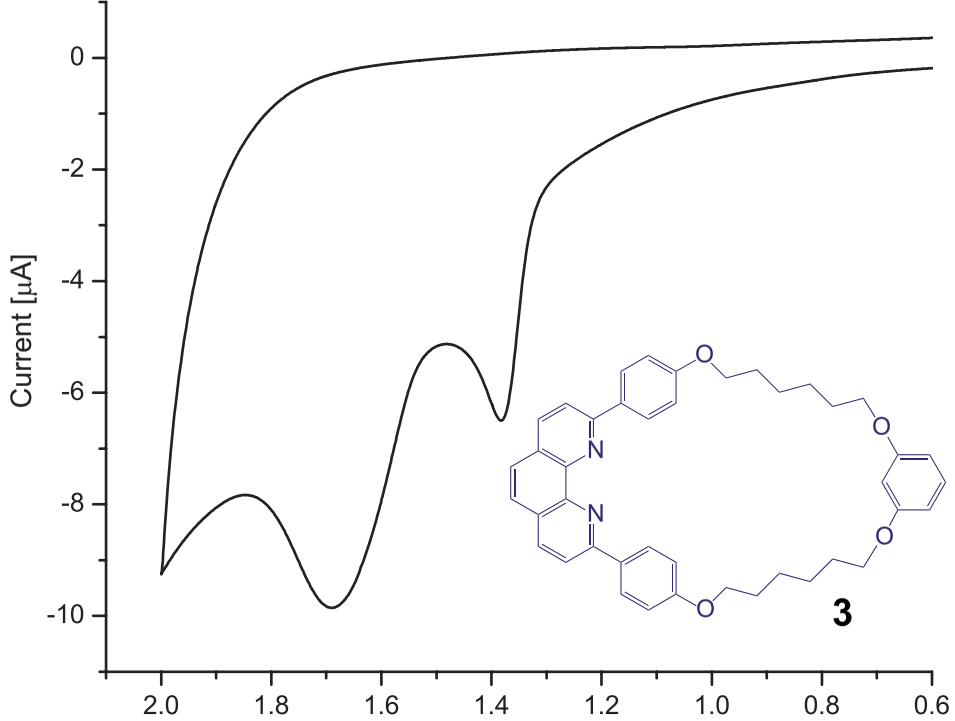

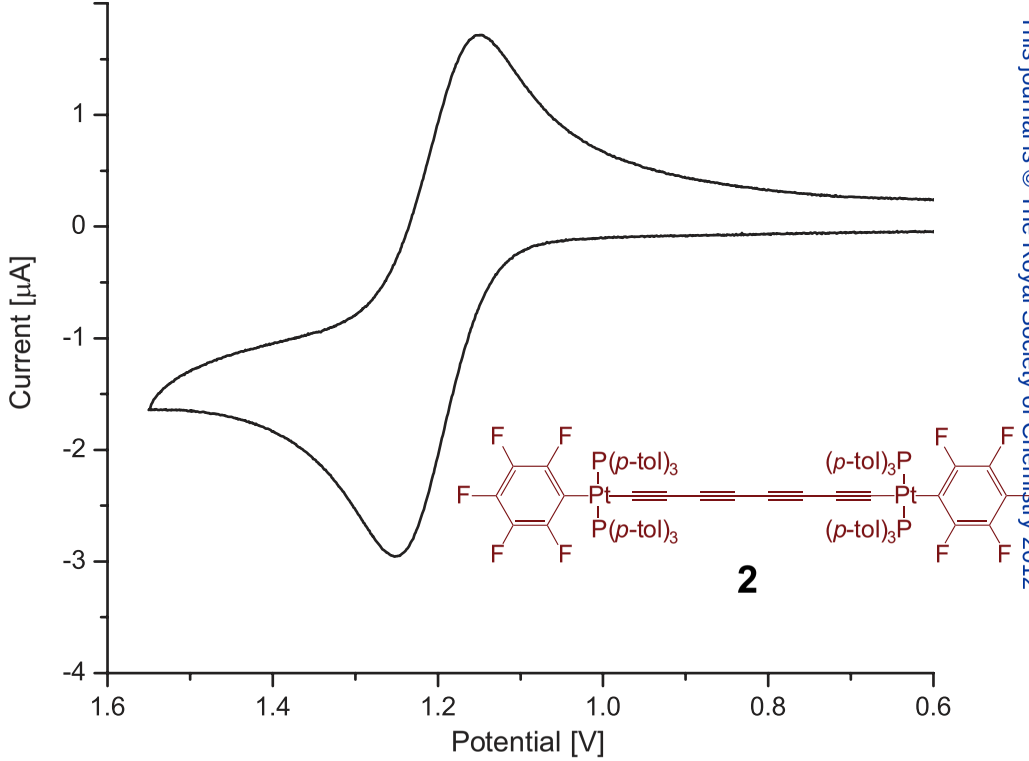

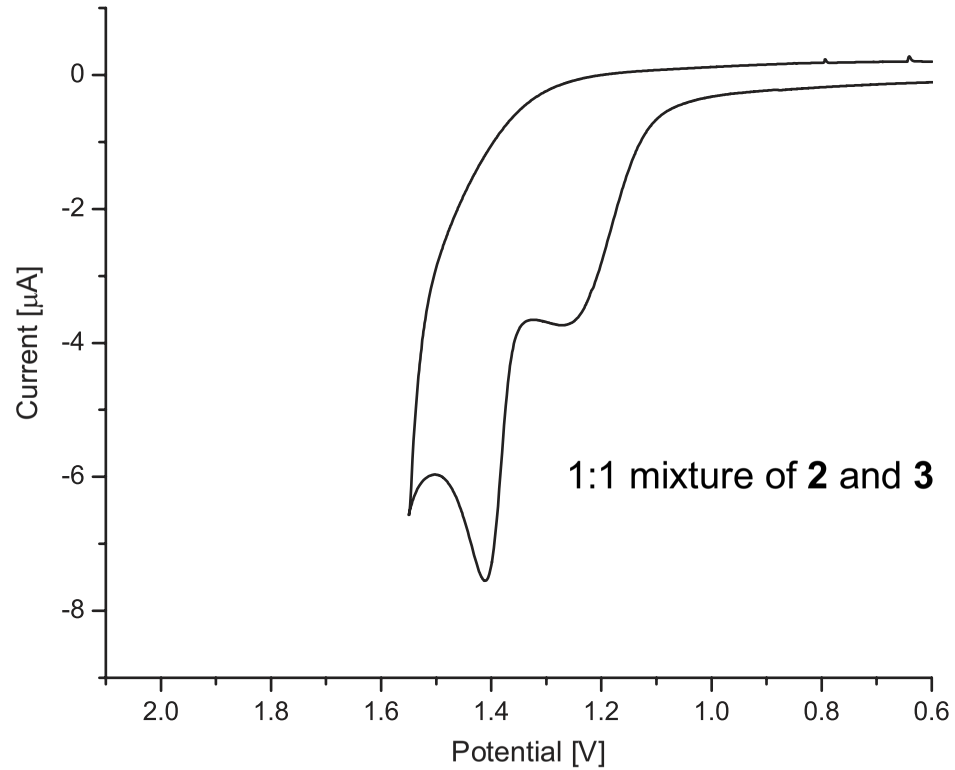

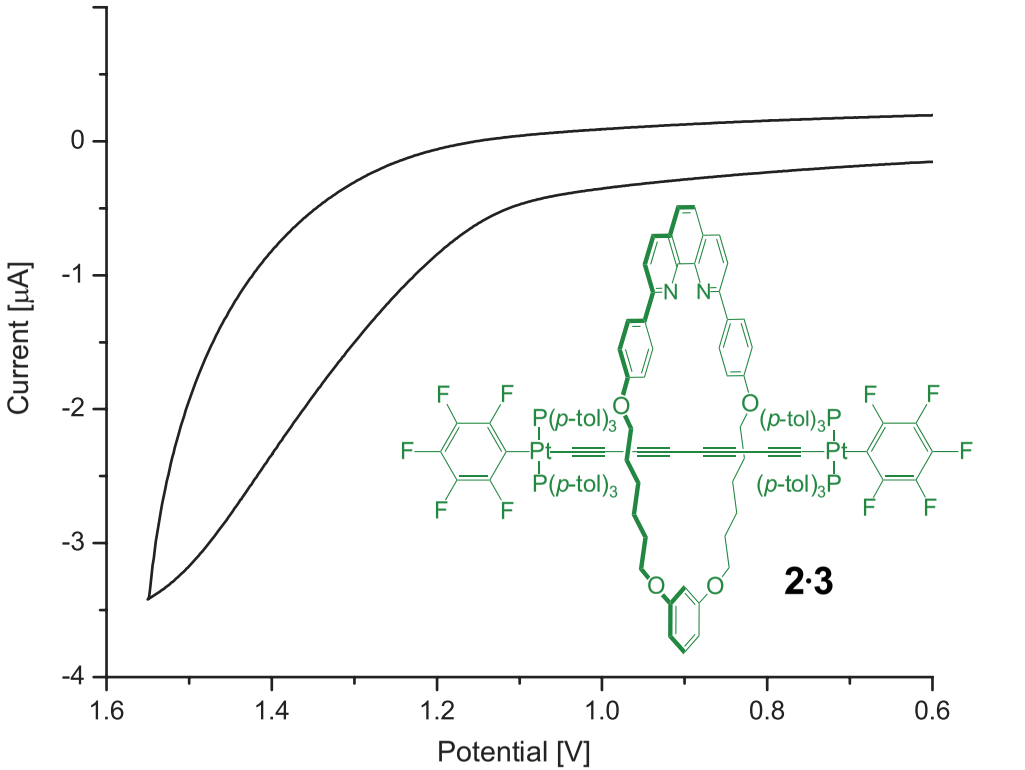

Figure s4. Cyclic Voltammograms.